Title:
Dynamic Modeling and Experimental Validation of a Robotic Whip

Authors:
Thomas M. Kwok, mfkwok@mae.cuhk.edu.hk, The Chinese University of Hong Kong
Yong Zhong, biezhon@nus.edu.sg, National University of Singapore
Ruxu Du, rdu@mae.cuhk.edu.hk, The Chinese University of Hong Kong

Keywords:
Dynamics, soft robotics, Pseudo-Rigid-Body Model (PRBM), whip.

DOI: 10.14733/cadconfP.2018.47-53

Introduction:
Whip is a common tool that has been used for thousands of years. It has several distinct advantages over other rigid tools, such as highly flexible, light weight, under actuation, and capable of amplifying velocity, acceleration and force. With advanced robotic technology, can we make a robotic whip? From a technical point of view, a whip can be considered as a soft robot that can deform continuously. However, owing to the large number of degree-of-freedom and under actuation, such a robot is very difficult to control. In fact, whip usually follows chaotic motion. Therefore, to understand its dynamics is essential.

A whip can be considered as a flexible beam. It is known that a beam can be modeled by the Bernoulli-Euler beam theory when its deflection is small. Though, when the deflection is large, non-linear models must be adopted. To solve the non-linear model, the commonly used methods include Finite Element Analysis (FEA) and Large Deflection Theory. While these methods are effective, they demand for heavy computation load and often suffer from large errors. In recent year, the so-called Pseudo-Rigid-Body Model (PRBM) is developed [2]. Examples include Howell and Midha's 1R PRBM [3], Su's 3R PRBM [4], Yu's 2R PRBM [7] and Yu's 5R PRBM [8]. These examples demonstrate how to use a series of rigid links and revolute joints to approximate the large deflection of a flexible beam. To have an accurate approximation, PRBMs need a number of parameters. As a result, multiple parameter optimization is required and modeling errors could be significant. For example, Zhong and *et al* used a 3R PRBM to model the compliant tail of their robot fish [9]. The maximum error is around 19%.

In this paper, we use PRBM to model the dynamics of a robotic whip. The experiment validation is also included.

Main Idea:
The experiment setup and geometric linearity assumption
As shown in Fig. 1(a)., 1R PRBM [3] uses two pseudo rigid links, as well as one revolute joints, represented in black, to approximate a beam bending to an arc, represented in red. The model has two sets of parameters: the characteristic radius factors, γ_1, γ_2, and the torsional spring stiffness coefficient, K_θ. The torsional spring constant, K, can be computed using the following formula:

$$K = \gamma_2 K_\theta \frac{EI}{L} \tag{1}$$

where E the modulus of elastic, I the moment of inertia and $L = \gamma_1 L + \gamma_2 L$ the length of the whip. With Eqn. (1), the pseudo-rigid-body angle, θ, can then be calculated based on the applied torque, T:

$$T = K\theta \tag{2}$$

Similarly, as shown in Fig. 1(b)., 2R PRBM is made of three links and two joints, $\gamma_1 L$, $\gamma_2 L$, $\gamma_3 L$ and θ_1, θ_2. It would require four characteristic parameters, $K_{\theta 1}$, $K_{\theta 2}$, γ_2 and γ_3, to compute K_1 and K_2. In general,

*N*R PRBM consists of 2*N* parameters, where *N* is referred as the order of the PRBM.

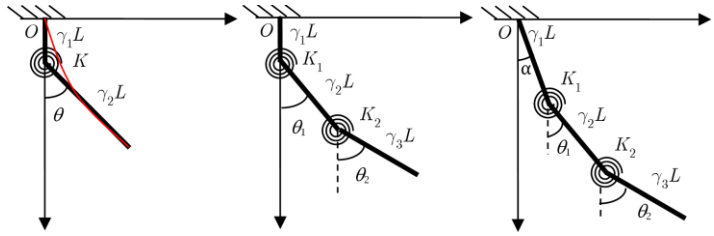

Fig. 1: Illustration of PRBM: (a) 1R PRBM, (b) 2R PRBM, (c) 2R PRBM with a rotation angle, α.

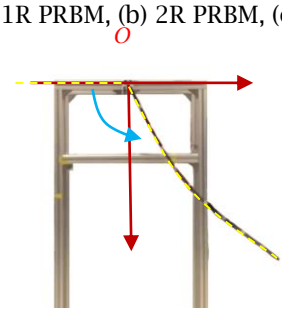

Fig. 2: The experiment setup for testing the robotic whip in free fall motion. The red arrows are the 2D coordinate, the yellow dash lines show whip positions, and the blue arrow indicates the moving direction. In the experiment, we assume friction of joint at *O* is negligible.

Geometry dimension and properties	*Value*
Radius (m)	0.005
Length (m)	1
Mass (kg)	0.15
Elastic modulus (GPa)	0.0229

Tab. 1: The dimensions and properties of whip.

Note that the robotic whip has the same geometrical dimension and material properties throughout the entire length. Having a similar assumption with Saggere [6], we assume that *K* is the same for all joints. With constant K_θ and γ, *K* is modified as Eqn. (3). Hence, K_θ is the only parameter that needs to be found in optimization.

$$K_i = K_\theta \frac{EI}{\gamma L}, i = 1,2,...,N \tag{3}$$

Kinematic analysis

Depending on the required accuracy, the robotic whip can be modeled by various PRBM models with different orders. As an example, Fig. 1(c). shows the 2R PRBM model with the reference frame set at the center, *O*. Its kinematical model can be derived directly. It can be shown that the center positions of the pseudo rigid links, **P**, are as follows:

$$\mathbf{P}_1 = \begin{bmatrix} \frac{\gamma_1 L}{2}\sin\alpha \\ \frac{\gamma_1 L}{2}\cos\alpha \end{bmatrix}, \quad \mathbf{P}_2 = \begin{bmatrix} \gamma_1 L\sin\alpha + \frac{\gamma_2 L}{2}\sin\theta_1 \\ \gamma_1 L\cos\alpha - \frac{\gamma_2 L}{2}\cos\theta_1 \end{bmatrix}, \quad \mathbf{P}_3 = \begin{bmatrix} \gamma_1 L\sin\alpha + \gamma_2 L\sin\theta_1 + \frac{\gamma_3 L}{2}\sin\theta_2 \\ \gamma_1 L\cos\alpha - \gamma_2 L\cos\theta_1 - \frac{\gamma_3 L}{2}\cos\theta_2 \end{bmatrix}, \mathbf{P}_i \in \mathbb{R}^2, i = 1,2,3 \tag{4}$$

where, α is the rotation angle; θ_1 and θ_2 are the angles of revolute joint; $\gamma_1 L$, $\gamma_2 L$, $\gamma_3 L$ are the length of the pseudo rigid links with $\gamma_1 = \gamma_2 = \gamma_3 = 1/3$; subscript i = 1, 2, 3 is used to index the revolute joints. Moreover, their linear velocities (**v**) at the center of mass of links are:

$$\mathbf{v}_i = \frac{d}{dt}\mathbf{P}_i, \mathbf{v}_i \in \mathbb{R}^2, \mathbf{P}_i \in \mathbb{R}^2, i = 1,2,3, \tag{5}$$

The angular velocities (w) of the pseudo rigid links are:

$$w_\alpha = \frac{d}{dt}\alpha \text{ , } w_i = \frac{d}{dt}\theta_i, i = 1,2 \tag{6}$$

Dynamic Analysis

The dynamical model can be derived by using Euler-Lagrange equation [5]. The Lagrangian of the robotic whip is:

$$L = T - V \tag{7}$$

where,

$$T = \sum_{i=1}^{3} \frac{1}{2} m_i \mathbf{v}_{\mathbf{C}_i}{}^T \mathbf{v}_{\mathbf{C}_i} + \frac{1}{2} \mathrm{I}_C \, w_\alpha{}^2 + \sum_{j=1}^{2} \frac{1}{2} \mathrm{I}_C \, w_j{}^2 \tag{8}$$

$$V = \sum_{i=1}^{3} m_i g h_i + \frac{1}{2} K_1 (\theta_1 - \alpha)^2 + \frac{1}{2} K_2 (\theta_2 - \theta_1)^2 \tag{9}$$

$$I_C = \frac{1}{4} m_i r_i^2 + \frac{1}{12} m_i \gamma_i{}^2 L^2 \tag{10}$$

where, m, I_C, r and g are the mass, the moment of inertia, the radius of robotic whip and the gravity respectively. The three equations of motion for the modified 2R PRBM are:

$$\begin{cases} \frac{d}{dt}\frac{\partial L}{d\dot{\alpha}} - \frac{\partial L}{d\alpha} + \frac{\partial C_H}{d\dot{\alpha}} = 0 \\ \frac{d}{dt}\frac{\partial L}{d\dot{\theta}_1} - \frac{\partial L}{d\theta_1} + \frac{\partial C_H}{d\dot{\theta}_1} = 0 \\ \frac{d}{dt}\frac{\partial L}{d\dot{\theta}_2} - \frac{\partial L}{d\theta_2} + \frac{\partial C_H}{d\dot{\theta}_2} = 0 \end{cases} \tag{11}$$

where C_H is hysteresis damping of material, which is the only damping term in this model. The air resistance is not considered as it is negligible when comparing with hysteresis damping of material. The equivalent viscous damping constant is $c_{eq} = \eta\sqrt{Km}$, where $\eta = \frac{4 \times 10^{-2}}{E}$ is the loss coefficient for polymers [1].

$$C_H = \frac{1}{2} c_{eq} (\dot{\theta}_1 - \dot{\alpha})^2 + \frac{1}{2} c_{eq} (\dot{\theta}_2 - \dot{\theta}_1)^2 \tag{12}$$

The aforementioned model is implemented using Mathematica©. Fig. 3. shows a simulation example, in which the robotic whip is modeled by 2R PRBM. At t = 0, the whip is released from the horizontal plane and follows a free fall. Thus, all initial joint angles and angular velocities are set to be zero in this example. Fig. 3. shows 10 positions of the whip, each being Δt = 0.1 s apart.

$t = 0.9$

Parameter Optimization for finding the spring constant

As mentioned above, the spring constants for all the joints are the same and hence, there is only one unknown parameter, K_θ. The objective of the optimization is to find K_θ that minimizes the average relative error of the positions of 11 points on whip between the experiment and the simulation results, where 11-point positions on whip include base, 9 joint positions and tip position of whip.

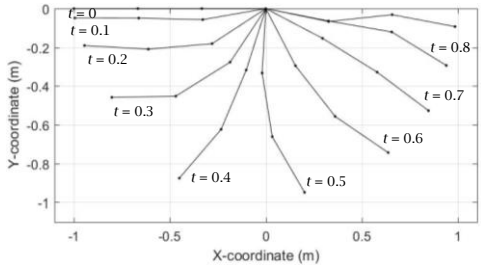

Fig. 3: A simulation example, in which the robotic whip is modeled by 2R PRBM with $K_\theta = 0.001$. In this example, the robotic whip follows a free fall.

The robotic whip position data are captured using a video camera. The result is as follows.

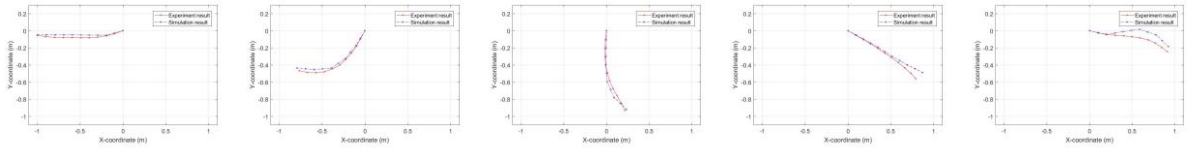

Fig. 4: The comparison of experiment and simulation results. The experiment is conducted using the aforementioned setup. The model is 4R PRBM with $K_\theta = 0.0001$. Point positions: (a) At t=0.1s, (b) At t=0.3s, (c) At t=0.5s, (d) At t=0.7s, (e) At t=0.9s.

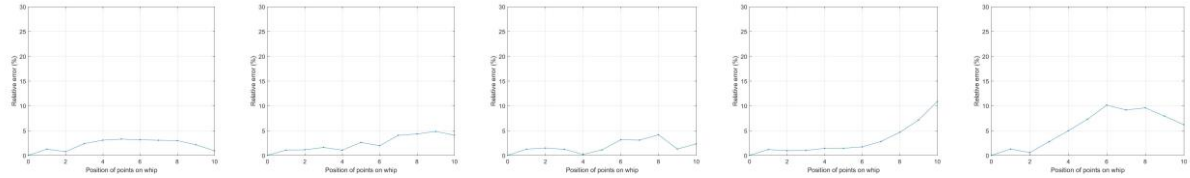

Fig. 5: Relative errors at different point positions: (a) At t=0.1s, (b) At t=0.3s, (c) At t=0.5s, (d) At t=0.7s, (e) At t=0.9s.

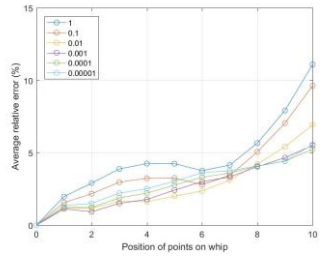

Fig. 6: The average relative error between the experiment and the simulation at different positions with $K_\theta = 1$, 0.1, 0.01, 0.001, 0.0001 and 0.00001, respectively.

By comparing the result with different stiffness coefficients in Fig. 6., the optimal stiffness coefficient for 4R PRBM is $K_\theta = 0.0001$. In the following experiment, the optimal stiffness coefficient for 1R, 4R, 9R, 19R, 29R, 39R, 49R, 59R, 69R, 79R, 89R and 99R PRBM will be found.

Experimental Validation

A large number of experiments have been conducted to validate the presented model. Two sets of experiment results are presented herein.

For experiment 1, analyzing the accuracy of different number of revolute joints in PRBM. Fig. 7. shows the average relative error using different number of revolute joints in PRBM. Fig. 8. shows the

comparison of the average relative error of different number of revolute joints with corresponding optimal K_θ.

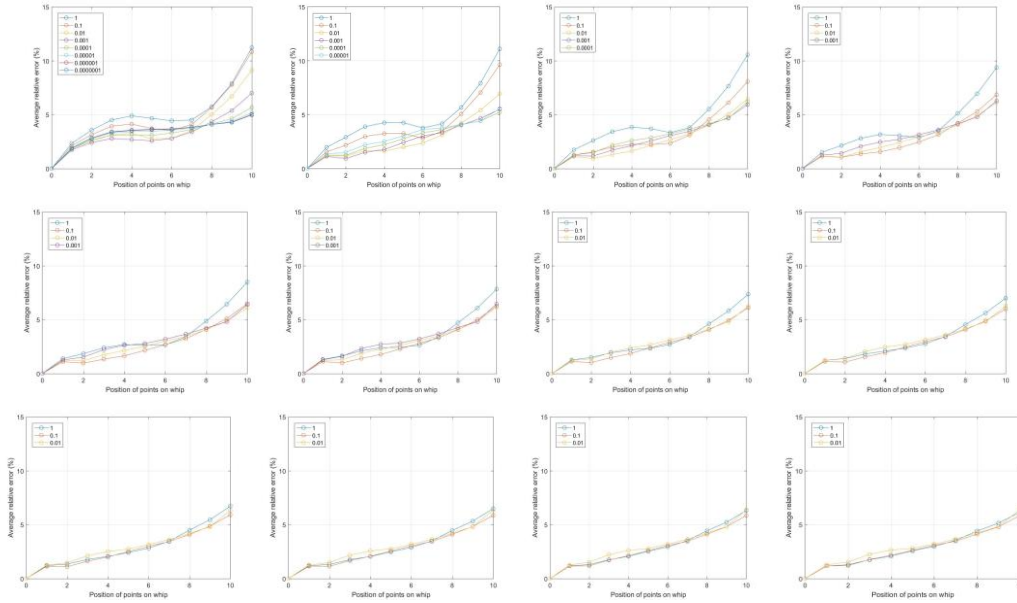

Fig. 7: The average relative error between the experiment and the simulation at different positions with different K_θ : (a) 1R, (b) 4R, (c) 9R, (d) 19R, (e) 29R, (f) 39R, (g) 49R, (h) 59R, (i) 69R, (j) 79R, (k) 89R, (l) 99R.

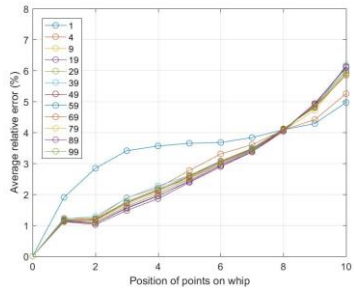

Fig. 8: The average relative error of 1R, 4R, 9R, 19R, 29R, 39R, 49R, 59R, 69R, 79R, 89R and 99R between the experiment and the simulation at different positions with optimal K_θ.

Number of R	*Optimal K_θ*	*K*	*Sum of squares of average relative error (%)*
1	1×10^{-7}	2.07×10^{-9}	137.23
4	0.0001	5.18×10^{-6}	106.65
9	0.001	1.04×10^{-4}	111.92
19	0.01	2.07×10^{-3}	112.45
29	0.01	3.11×10^{-3}	115.18
39	0.01	4.15×10^{-3}	118.48
49	0.1	0.05	111.54
59	0.1	0.06	111.27
69	0.1	0.07	111.32

79	0.1	0.08	111.72
89	0.1	0.09	112.41
99	0.1	0.10	113.26

Tab. 2: The sum of squares of average relative error between the experiment and the simulation at different positions with optimal K_θ.

As shown in Fig. 8. and Tab. 2., 4R PRBM has the best fit. Although the maximum average relative error is small when less revolute joints are applied, the sum of squares of average relative error is significantly large. It implied that the shape of whip is not accurate when smaller number of joints is used. This may be attributed to the fact that when less revolute joints are used, the degree of freedom is insufficient in describing the dynamics of the whip. Thus, number of joint should be larger than 1 to have an accurate result. On the other hand, when large number of revolute joints are used, the numerical error may take a toll. Therefore, 4R PRBM is preferred for modeling in this case due to a smaller computation load and higher accuracy.

For experiment 2, analyzing the relative error of the 4R PRBM for the free fall condition. Fig. 9. shows a comparison between the simulation and the experiment results. As shown in Fig. 9(a)., the maximum relative error is 11.08% while as shown in Fig. 9(b)., the average relative error is about 5.25%. This indicates that the 4R PRBM with a constant torsional spring can model the robotic whip with good accuracy.

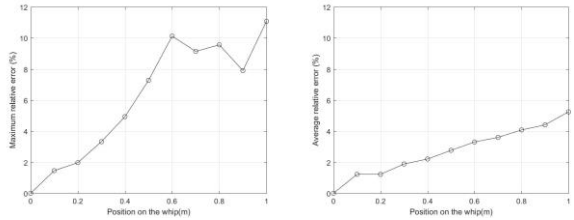

Fig. 9: A comparison between the experiment and the simulation using 4R PRBM with $K_\theta = 0.0001$: (a) Maximum relative error, (b) Average relative error.

Conclusions:

This paper presents a study on robotic whip. Based on the discussions above, following conclusions can be drawn:

- Whip can be modeled by *N*R PRBM with the same torsional spring constant for all joints. With the increase of the order, *N*, the modeling accuracy increases.
- The accuracy of 4R PRBM is good enough for modeling. The maximum relative error between the simulation and the experiment results is 11.08% and the average relative error is 5.25%. The error may be attributed to the fact that PRBM does not consider damping.

In the future, two topics will be further investigated. The first one is to investigate the chaotic behavior of robotic whip which will occur when the time goes by. The second topic is to control robotic whip to reach specific target with specific speed.

Acknowledgements:

We gratefully thank the Hong Kong Research Grant Council Ref. no. 14204417 for financial support.

References:

[1] Ashby, M. F.: Mechanical Selection in Mechanical Design, Elsevier Science, 2004.
[2] Howell, L. L.: Compliant Mechanisms, Wiley-Interscience, Canada, 2001.

[3] Howell, L. L.; Midha A.: Parametric Deflection Approximations for End-Loaded, Large- Deflection Beams in Compliant Mechanisms, ASME Journal of Mechanical Design, 117(1), 1995, 156-165. https://doi.org/10.1115/1.2826101
[4] Su, H. J.: A load independent pseudo-rigid-body 3R model for determining large deflection of beams in compliant mechanisms, International Design Engineering Technical Conferences and Computers and Information in Engineering Conference, ASME, 2, 2008, https://doi.org/10.1115/DETC2008-49041
[5] Shabana, A.A.: Dynamics of multibody systems, Cambridge University Press, New York, NY, 2013.
[6] Saggere, L.; Kota, S.: Synthesis of Planar, Compliant Four-Bar Mechanisms for Compliant-Segment Motion Generation. Trans. of ASME, J. of Mechanical Design, 123(4), 1999, 535-541. https://doi.org/10.1115/1.1416149
[7] Yu, Y. Q.; Feng, Z. L.; Xu, Q. P.: A pseudo-rigid-body 2R model of flexural beam in compliant mechanisms, Mechanism and Machine Theory, 55, 2012, 18-33. https://doi.org/10.1016/j.mechmachtheory.2012.04.005
[8] Yu, Y. Q.; Zhu, S. K.: 5R pseudo-rigid-body model for inflection beams in compliant mechanisms, Mechanism and Machine Theory, 116, 2017, 501-512. https://doi.org/10.1016/j.mechmachtheory.2017.06.016
[9] Zhong, Y.; Li, Z.; Du, R.: A Novel Robot Fish With Wire-Driven Active Body and Compliant Tail, IEEE/ASME Transactions on Mechatronics, 22(4), 2017, 1633-1643. https://doi.org/10.1109/TMECH.2017.2712820